Talanta 307 (2026) 129761

Contents lists available at ScienceDirect

Talanta

journal homepage: www.elsevier.com/locate/talanta

Multifunctional potentiostat for static and fluidic electrochemical sensing: Validation and application to detection of *Pseudomonas aeruginosa*

Elisa Paialunga [a,1], Rocco Cancelliere [b,1], Antonio Licheri [a], Cosimo Micelli [c], Antonio Ceccarelli [d], Giulia Sarpi [a], David Albano [e,f], Benedetta Brugnoli [e,f], Iolanda Francolini [f], Laura Micheli [a,*,2], Giuseppina Rea [e,**,2]

[a] Department of Chemical Science and Technologies, University of Rome Tor Vergata, Via Della Ricerca Scientifica, 00133, Rome, Italy
[b] Technologies and Devices for Electrochemical Storage (TERIN-DEC-ACEL), Italian National Agency for New Technologies, Energy and Sustainable Economic Development (ENEA), Via Anguillarese 301, 00123, Rome, Italy
[c] KleisTEK, Advanced Electronic Systems, Via Reginaldo Pirano 15, 70043, Monopoli (Bari), Italy
[d] Laboratorio di Analisi Agroalimentare Sana srl, Corso Lazio 17, Frosinone, 03100, Italy
[e] Institute of Crystallography, CNR (National Research Council), Via Salaria Km 29.300, 00015, Monterotondo Stazione (Rome), Italy
[f] Department of Chemistry, Sapienza University, P.le Aldo Moro 5, 00185, Rome, Italy

ARTICLE INFO

Keywords:
Integrated potentiostat
Static and fluidic sensing
Label-free biosensors
Pseudomonas aeruginosa
Lab-on-field applications

ABSTRACT

This work reports the development and analytical validation of FACILE 2.0, a portable multifunctional potentiostat designed for electrochemical measurements under both static and microfluidic configurations. The platform integrates a compact electrochemical interface, embedded single-board computer, touchscreen control, and programmable flow handling, enabling autonomous execution of cyclic voltammetry, square wave voltammetry, chronoamperometry, and electrochemical impedance spectroscopy. Analytical performance was first validated using benchmark reversible redox systems and electroactive species exhibiting different electron-transfer kinetics. Under static conditions, calibration studies demonstrated high linearity (R^2 up to 0.999), repeatability of 8% (RSD), and a limit of detection of 0.7 μM for representative redox probes, values comparable to commercial benchtop and portable potentiostats. Correlation analyses confirmed strong agreement in current response and extracted electrochemical parameters across different techniques. Measurements performed in fluidic mode further demonstrate stable and reproducible responses under controlled flow conditions. Following electrochemical validation, FACILE 2.0, was applied as a representative case study to a label-free immunosensor for the detection of *Pseudomonas aeruginosa* in untreated tap water. Using square wave voltammetry, the system achieved a limit of detection of 1000 CFU/mL (RSD <10%, n = 5), with high specificity against non-target microorganisms (<10% interference).

With a compact footprint (W32 x D18 x H5 cm), low power consumption (<15W maximum), and complete portability (1.93 kg), FACILE 2.0 provides a robust, scalable and field-deployable solution for a broad range of electrochemical applications, including environmental monitoring, industrial quality control, materials research, teaching laboratories, and decentralized biosensing applications.

* Corresponding author
** Corresponding author
E-mail addresses: elisa.paialunga@uniroma2.it (E. Paialunga), rocco.cancelliere@enea.it (R. Cancelliere), antonio.licheri@uniroma2.eu (A. Licheri), c.micelli@kleistek.com (C. Micelli), antonio.ceccarelli@sanasrl.it (A. Ceccarelli), giulia.sarpi@alumni.uniroma2.eu (G. Sarpi), david.albano@uniroma1.it (D. Albano), benedetta.brugnoli@uniroma1.it (B. Brugnoli), iolanda.francolini@uniroma1.it (I. Francolini), laura.micheli@uniroma2.it (L. Micheli), giuseppina.rea@cnr.it (G. Rea).
[1] These two authors contributed equally as first authors.
[2] These two authors contributed equally as corresponding and last name authors.

https://doi.org/10.1016/j.talanta.2026.129761
Received 19 December 2025; Received in revised form 28 March 2026; Accepted 1 April 2026
Available online 2 April 2026

1. Introduction

Electrochemical (Bio)sensors (EBs) have emerged as powerful analytical tools for the rapid, low-cost detection of chemical and biological targets, offering applications across medical diagnostics, environmental surveillance, and food safety [1,2]. Their success is driven by the unique combination of high sensitivity, compatibility with miniaturized electronics, and potential for point-of-need deployment. At the core of these systems is the potentiostat, which enables precise control and acquisition of electrochemical signals [3,4].

Beyond biosensing applications, potentiostats play a fundamental role in electrochemical research and education, including the characterization of redox systems, corrosion studies, battery and energy storage research, electrode material development, and analytical chemistry training. The availability of compact, affordable, yet high-performance platforms is therefore critical not only for pathogen detection but also for academic teaching laboratories and decentralized industrial quality control settings. Despite considerable progress in biosensing technologies, the architecture of conventional potentiostats remains a key bottleneck. Most commercial systems are bulky, expensive, and designed for static, laboratory-based measurements, conditions that are incompatible with the demands of portable, real-time, or continuous sensing [3,5]. These limitations hinder the broader adoption of EBs in resource-limited settings and real-time decision-making contexts [6–9].

In recent years, significant efforts have been focused on developing compact, portable potentiostats that combine high analytical performance with low power consumption and modular functionality [5,10,11]. However, few existing solutions offer seamless integration of multiple sensing modes (static and fluidic), embedded data processing, and real-time usability, especially in systems designed for real-world analysis in complex samples across environmental, biomedical, and industrial domains [8,12–15].

In this context, we present FACILE 2.0, a multifunctional, portable potentiostat developed to support electrochemical (bio)sensing in both static and microfluidic configurations. FACILE 2.0 integrates an embedded single-board computer, touchscreen interface, onboard conductivity sensing, and a modular fluidic system. The platform supports high-resolution voltammetric and impedance techniques while maintaining compactness and affordability, offering a field-deployable alternative to commercial-grade instruments. Before its application in a case of study, the FACILE 2.0's electrochemical performances were demonstrated by comparison with measurements of cyclic and square wave voltammetry (CV and SWV, respectively), electrochemical impedance spectroscopy (EIS), and chronoamperometry (CA) of the same electroactive probes: two reversible redox couple of potassium ferri/ferrocyanide $[Fe(CN)_6]^{3-/4-}$, and hexaammineruthenium(III/II) $[Ru(NH_3)_6]^{2+/3+}$, and two biologically relevant species, ascorbic acid (AA) and dopamine (DA). The first two redox systems, known for their well-defined and reversible electrochemical behavior, were used as benchmark references. Comparative measurements were conducted using commercial devices such as the Autolab PGSTAT 12 (Metrohm, NL), PalmSens 4.0 (PalmSens, NL), and EmStat *Blue* (PalmSens, NL).

As a representative case study, FACILE 2.0 was coupled with an electrochemical immunosensor developed for monitoring *Pseudomonas aeruginosa* (*P. aeruginosa*) presence in tap water, serving as a case study to demonstrate the application of the proposed electrochemical system.

P. aeruginosa is a Gram-negative bacterium classified by the World Health Organization (WHO) as a high-priority pathogen due to its virulence, biofilm formation, and intrinsic antibiotic resistance [16–18]. *P. aeruginosa* is a leading cause of hospital-acquired infections, particularly in Intensive Care Units (ICUs) and among immunocompromised patients [19–21], and poses additional risks in aquaculture and contaminated food or water supplies [22–26]. Although the presence of *P. aeruginosa* in potable water does not always pose an immediate concern, it may still warrant attention, particularly under specific circumstances. Generally, a low presence of this bacterium in water is considered physiological, while a high concentration could indicate a hygiene problem in the supply system [27].

Traditional detection methods of this bacteria, including culture-based assays and automated biochemical platforms, offer high specificity but are time-consuming, costly, and require sampling and analysis in laboratory [28–30]. Molecular diagnostics, including Polymerase Chain Reaction (PCR) and Loop Mediated Isothermal Amplification (LAMP), improve sensitivity but require specialized equipment and trained personnel [31,32]. In contrast, electrochemical immunosensors, particularly those using label-free detection strategies, offer a portable, specific, and rapid alternative for *in situ* analyses, specific, and rapid alternative to the traditional tools [33].

In this work, we report the development of a label-free immunosensor based on biochar-modified screen-printed electrodes (SPEs) for the detection of *P. aeruginosa* and its application with the FACILE 2.0 platform using SWV, as an electrochemical technique. With this tool, detection limits of 170 CFU/mL in buffer and 1000 CFU/mL in tap water without any pretreatment were obtained, respectively, and reliable reproducibility under both controlled and real sample conditions.

This study demonstrates that FACILE 2.0 offers a versatile, scalable solution for field-deployable biosensing, bridging the gap between benchtop performance and point-of-need monitoring. The combined use of sustainable materials, embedded electronics, and fluidic automation positions FACILE 2.0 as a promising tool for next-generation electrochemical sensing platforms.

2. Materials & methods

2.1. Reagents and solutions

All chemicals from commercial sources were of analytical grade. Sodium chloride (NaCl), potassium chloride (KCl) sodium dihydrogen phosphate (NaH_2PO_4), disodium hydrogen phosphate (Na_2HPO_4), ethanol (99%), ethanolamine, Tween20, potassium ferricyanide, potassium ferrocyanide trihydrate, hexaammineruthenium(III) chloride, hexaammineruthenium(II) chloride, ascorbic acid, dopamine, 2-(N-morpholino)ethanesulfonic acid (MES, 99%), N-hydroxysuccinimide (NHS, 98%), and 1-ethyl-3-(3-dimethylaminopropyl) carbodiimide (EDC, 97%) were purchased from Sigma-Aldrich (Darmstadt, DE). Anti-Rabbit IgG (whole molecule) antibody produced in sheep, and Polyclonal *Anti-P. aeruginosa* antibody produced in rabbit were purchased from Sigma-Aldrich (Darmstadt, DE). All microbial strains, including *P. aeruginosa*, *Escherichia coli* (*E. coli*), *Staphylococcus aureus* (*S. aureus*), and *Hepatitis* A virus, each with a known titer (CFU/mL), were provided by SANA srl (Frosinone, IT). All antibodies were aliquoted and stored at 4 °C for immediate use or at −20 °C for long-term storage. Buffer solutions included phosphate-buffered saline (PBS; 3.88 mM NaH_2PO_4, 6.12 mM Na_2HPO_4, 137 mM NaCl, 2.5 mM KCl, pH 7.4) and 100 mM MES buffer (pH 6.0). All redox probes and spiked solutions of *P. aeruginosa* were prepared in PBS, unless otherwise specified.

2.2. Preparation of biochar dispersion and modification of SPEs

Biochar was purchased from Bi-biochar srl (Biella, IT) and supplied with a technical sheet detailing its composition and characteristics. SPEs were home-made at the University of Rome Tor Vergata [34] using a DEK 245 screen-printing machine (Weymouth, UK). The graphite-based working electrode was modified by applying the previously prepared biochar suspension in ethanol/H_2O solution (1:3, v/v) to reach a final concentration of 1 mg/mL, followed by homogenization using an ultrasonic processor (UP200St Hielscher, Teltow, DE) for 30 min at 70% amplitude. The resulting biochar-modified SPEs (Bio-SPEs) were then employed for all measurements and the development of the immunosensor.

2.3. Apparatus

To test the electrochemical performances of the proposed prototype, FACILE 2.0 (detailed in Section 3.1) several electrochemical analyses were carried out, including CV, SWV, CA and EIS, using various redox probes: $[Fe(CN)_6]^{3-/4-}$, $[Ru(NH_3)_6]^{2+/3+}$, AA and DA. The results were then compared with data obtained from two commercial portable instruments, PalmSens 4.0 (PSTrace 10, software) and EmStat *Blue* (PSTrace 10, software), both manufactured by PalmSens (NL), as well as the benchtop instrument computer-controlled system Autolab PGSTAT 12 (Metrohm, NL) equipped with GPES software (Ecochemie, NL). As a case study, FACILE 2.0 was employed for the detection of *P. aeruginosa* in water using a label-free electrochemical immunosensor, based on the $[Fe(CN)_6]^{3-/4-}$ redox probe (see Section 2.4). The measurements were compared with those obtained using the PalmSens 4.0, used as reference portable instrumentation.

2.4. Preparation of label-free electrochemical immunosensor for *P. aeruginosa*

The working electrode of Bio-SPEs was chemically activated using an aqueous solution containing EDC (4 mM) and NHS (5 mM) dissolved in 100 mM MES buffer (pH 6.0) and incubated in the dark at room temperature for 20 min to promote amide bond formation. For the pre-coating step, chemically activated Bio-SPEs were incubated with 5 μg/mL of rabbit *anti*-IgG antibody (secondary antibody – Ab_{II}) solution in 10 mM PBS (pH 7.4), and then incubated overnight at 4 °C. Subsequently, a blocking step was performed by with the addition 6 μL of a 2% ethanolamine (ETA) solution in 10 mM PBS (pH 7.4) on the working electrode and incubating for 60 min at room temperature. During the coating step, 2.5 μg/mL of polyclonal primary *anti-P. aeruginosa* antibody (Ab_I) solution in 10 mM PBS (pH 7.4) was incubated on the working electrode to enable selective recognition of the target antigen. A calibration curve was generated by incubating several concentrations of *P. aeruginosa* suspensions in 10 mM PBS (pH 7.4) (prepared by SANA srl, Frosinone - IT) (0, 10, 100, 1000, 2000, 5000, 15000, and 30000 CFU/mL) onto the surface of the functionalized immunosensor to complete the immunological chain with the recognition of the bacteria (target antigen) by its primary antibody. Each modified immune-Bio-SPE was incubated at room temperature for 25 min to allow specific binding between the bacterial antigens and the immobilized antibodies. After each deposition step, the electrode was washed three times with 100 μL of PBS to remove unbound material. The immunocomplex formation (the scheme is reported in Fig. 1) was investigated using SWV as electrochemical technique with a 10 mM potassium $[Fe(CN)_6]^{3-/4-}$ solution as a redox probe. All measurements were performed in quintuplicate (n = 5).

2.5. Preparation and analysis of tap water samples

Tap water samples were collected from the public water system of Frosinone (IT), where the laboratories of SANA srl are located. The water was used without any pretreatment, spiked with increasing concentrations of *P. aeruginosa*, and immediately analyzed without any pretreatment, following the matrix study reported in the previous work carried out for *Hepatitis A* virus [35,36].

2.6. Theoretical methods

Signal variations were calculated as the percentage change in current with respect to the maximum and minimum values obtained from the response curves. This parameter represents the relative change in the electrochemical signal in the presence versus the absence of the bacterial target (*P. aeruginosa*) and was calculated using the following expression:

$$I\% = \left(\frac{I_{measured} - I_{min}}{I_{MAX} - I_{min}}\right) \times 100 \quad \text{Eq. 1}$$

where $I_{measured}$ is the signal measured at a given target concentration, I_{min} is the minimum value of the current range, I_{MAX} is the maximum value of the current range. The response curve as a function of *P. aeruginosa* concentration was fitted using a four-parameter logistic model (4 PL), according to the Warwick method, previously applied in studies conducted by our group [2,37]. The limit of detection (LOD) and the limit of quantification (LOQ) were defined as the sum of the mean signal measured in the absence of *P. aeruginosa* and three or ten times the corresponding standard deviation, respectively. Various concentrations of *P. aeruginosa* were tested in quintuplicate. The working ranges were defined as the concentration windows corresponding to the transition from 20% to 80% of relative signal variation within the binding curves. To assess specificity, signal variations were expressed as signal change using the following formula:

$$Signal\ Gain = \left(\frac{I_{measured} - I_{blank}}{I_{target} - I_{blank}}\right) \times 100 \quad \text{Eq. 2}$$

where $I_{measured}$ represents the signal in the presence of a potential interferent, and I_{blank} is the average current measured in the absence of the target or any interfering species (negative control), and I_{target} is the average current measured in the presence of *Pseudomonas*.

3. Results and discussion

3.1. Description of the FACILE 2.0 prototype

We have developed FACILE 2.0, a portable analytical platform that integrates electrochemical multi-transduction capabilities, modular architecture, microfluidic handling, and fast readout (Fig. 2, S1, S2). FACILE 2.0 supports dual operational modes: static, for batch or endpoint measurements, and dynamic, for continuous flow-based assays. This dual-mode functionality significantly enhances the platform's adaptability across a broad range of analytical scenarios, including both laboratory-based studies and *in situ* field applications. Beyond biosensing applications, this architecture enables the platform to function as a general-purpose electrochemical workstation suitable for method development, materials characterization, corrosion studies, energy storage research, and advanced teaching laboratories.

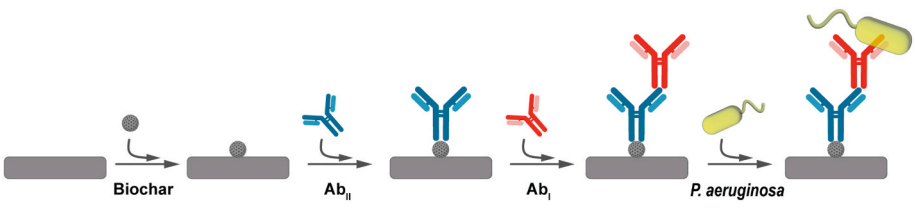

Fig. 1. Schematic representation of the *P. aeruginosa* immunosensor assembly. SPEs were first modified with biochar via drop-casting and subsequently activated with EDC/NHS chemistry to enable covalent immobilization of the secondary antibody (Ab_{II}). The primary antibody (Ab_I) was then immobilized to complete the immunological chain for target recognition. All immobilization steps were carried out in 10 mM PBS buffer (pH 7.4). Electrochemical measurements were performed by SWV using a 10 mM $[Fe(CN)_6]^{3-/4-}$ solution as a redox probe. All experiments were conducted in quintuplicate (n = 5).

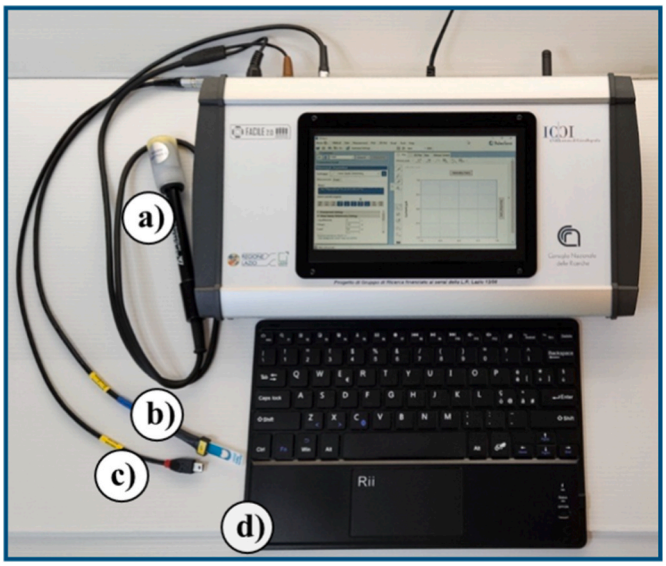

Fig. 2. Facile 2.0 potentiostat. The instrument is equipped with a) the conductivity probe model 2301T-F (Apera Instruments LLC, Columbus, Ohio, US) furnished with a temperature sensor); b) connecting cables for electrochemical measurements on electrodes from DropSens S.L. (Llanera, Spain) and, c) Micrux Technologies S.L. (Oviedo, Spain); d) Bluetooth keyboard.

At the core of the FACILE 2.0 system architecture is the EmStat *Blue* potentiostat module (Analog Devices Inc./PalmSens), a compact, dual-channel electrochemical interface capable of performing a comprehensive suite of electrochemical techniques, including amperometry, voltammetry, and EIS. The EmStat *Blue* can be operated via PSTrace 10, a widely adopted and user-friendly software platform that enables real-time control, data acquisition, and visualization. The use of PSTrace 10 facilitates direct benchmarking of FACILE 2.0 against established laboratory instrumentation, ensuring performance comparability and methodological consistency.

In addition to its electrochemical capabilities, the system has been extended to support conductivity measurements through the integration of a dedicated module composed of a microcontroller unit interfaced with a set of analog front-end daughter boards from Analog Devices. This subsystem was specifically configured for aqueous media characterization, aligning with common requirements in water quality monitoring and environmental sensing applications. This setup enables the measurement of conductivity, pH, and oxidation-reduction potential. FACILE 2.0 was hence supplied with the conductivity probe model 2301T-F equipped with a thermal probe (Apera Instruments, LLC; Columbus, Ohio, US).

A peristaltic pump was utilized to deliver the low flow rates required for microfluidic operations, with precise regulation achieved via a custom-developed control subsystem incorporating an STM32 microcontroller and a MOSFET-based power stage. The embedded firmware, specifically engineered for this application, enables precise flow control within a range of 5 µL/min to 10 mL/min, with a minimum step size of 5 µL/min. This architecture ensures accurate and reproducible flow modulation, supporting both continuous and discrete microfluidic protocols, as well as efficient priming and purging of fluidic lines connected to the experimental chamber. This functionality guarantees efficient sample transport, thereby maximizing mass transfer and ensuring optimal analyte interaction with the integrated biosensing elements. The embedded control software provides dynamic selection and execution of electrochemical analysis techniques, allowing method adaptation based on the specific analytical requirements. The platform's capability to perform high-sensitivity analyses on microvolumes is particularly advantageous in applications where sample availability is limited or when detecting analytes at trace concentrations. This level of analytical performance supports deployment in industrial production environments, where the system can operate as both an online and offline tool for real-time and batch-mode quality control of manufacturing matrices.

A key enhancement introduced in the FACILE 2.0 prototype is the integration of a dedicated Single Board Computer (SBC) as the central processing unit coupled with a 7-inch capacitive touch screen for local system interaction. The graphical user interface is managed via a Windows 10-based environment, providing a stable and flexible platform for executing measurement routines and system-level functions.

All configuration, control, and data management operations of the instrument can be executed locally through the integrated touchscreen interface, optionally supported by a Bluetooth keyboard. Additionally, full remote access and operation are enabled via Ethernet or Wi-Fi connectivity, allowing for seamless integration into laboratory or industrial network infrastructures.

The system architecture is modular, with the three primary functional subsystems interfaced to the SBC via USB communication channels, ensuring reliable data exchange and simplified hardware integration. An additional external USB port is provided for peripheral connectivity, such as USB flash drives or external storage devices, facilitating data export, firmware updates, or extended logging operations.

The integration of an internal CPU unit permits the development of the instrument's measurement and control software using a high-level programming environment, such as LabVIEW 2020. This graphical development framework supports rapid and efficient software development and code maintenance, thereby facilitating streamlined implementation and future scalability of the instrument's functionality through the integration of additional functions.

Software development and validation are performed on a standard development workstation, after which the compiled application is deployed to the SBC's internal storage via local network transfer or through removable media (e.g., USB drive). The update process is similarly straightforward, supporting both local and remote firmware/software upgrades, which enhances maintainability and supports long-term system evolution in both laboratory and industrial environments. The electronic components of the FACILE 2.0 system are housed within a custom-machined, screen-printed metal enclosure, which provides both mechanical robustness and electromagnetic shielding to minimize susceptibility to external electrical interference. Power is supplied either via a standard 12 V DC mains adapter (15 W maximum power consumption) or, for field-deployable applications, through an external 12 V battery pack, ensuring operational flexibility in both laboratory and off-grid environments.

Thermal characterization of the system was performed using an infrared thermographic camera to assess the operating temperatures of all critical subsystems, including the CPU unit. All components were confirmed to operate within nominal thermal specifications under standard working conditions (Fig. S3). Nevertheless, to enhance thermal management and maintain optimal airflow within the enclosure, a low-noise axial cooling fan (25 mm diameter) was integrated into the housing. Owing to its modular architecture and compatibility with standard three-electrode configurations, FACILE 2.0 can be readily employed in educational electrochemistry laboratories as a teaching instrument, as well as research environments requiring flexible electroanalytical experimentation. Its user-friendly interface lowers the technical barrier typically associated with advanced electrochemical instrumentation. Thanks to its compact footprint (W32 x D18 x H5 cm), and lightweight (1.93 kg), robust hardware architecture, and autonomous power capability, FACILE 2.0 is particularly suited for field-based analytical deployments. Its design incorporates both operational reliability and environmental resilience, making it a robust platform for on-site chemical and biochemical analyses across a range of industrial and environmental monitoring scenarios.

3.2. Electrochemical performance of FACILE 2.0 under static conditions

FACILE 2.0 supports a comprehensive suite of electrochemical techniques, including voltammetric, pulsed, amperometric, coulometric, and impedimetric modes, delivering performance on par with laboratory-grade instrumentation. Initially, to assess its physical/electrical performances, a conductivity test was performed; the correlated results are reported in SI (Table S1). Afterwords, to validate FACILE 2.0 analytical capabilities, CV, SWV, and CA were conducted under static conditions using both FACILE 2.0 (Fig. 3a-c) and commercial PalmSens 4.0 (Figs. S4 and S5), with the reversible redox couple $[Fe(CN)_6]^{3-/4-}$ across concentrations ranging from 0 to 20 mM. All measurements were performed in triplicate (n = 3) to ensure reproducibility. EIS, as a complementary technique, is discussed in detail in SI (Fig. S6).

To assess its reliability, the results of the proposed electrochemical platform were compared with those from commercial PalmSens 4.0 for the same concentrations of $[Fe(CN)_6]^{3-/4-}$ using the different electrochemical techniques. The measurements obtained with the two instruments revealed a strong correlation between them, as shown in Fig. 4, confirming that FACILE 2.0 provides reliable and comparable data to those generated by commercial potentiostats. The calibration curves for $[Fe(CN)_6]^{3-/4-}$ obtained (Fig. 3d-f) demonstrate high sensitivity, with coefficients of determination (R^2) of 0.999, 0.969, and 0.998, and slopes of 1.03, 3.30, and 0.11 for CV (Ip_A), SWV, and CA, respectively, and excellent signal reproducibility of the FACILE 2.0 instrumentation. The linear fitting functions for each technique are summarized in Table 1. Moreover, from the CV analysis, analytical parameters such as the ratio of anodic to cathodic peak current (Ip_A/Ip_C) and peak-to-peak separation (ΔE) were extracted.

To underline the analytical performance of FACILE 2.0, a correlation study was conducted. As shown in Fig. 4, alongside the data reported in Fig. 3g and h, the results demonstrate a high degree of agreement across all tested electrochemical techniques. The nearly overlapping response trends confirm the reliability of FACILE 2.0 in replicating voltammetric and chronoamperometric outputs with excellent reproducibility. These findings reinforce the robustness of the platform's analogue signal acquisition and processing architecture, establishing FACILE 2.0 as a credible and accurate tool for multiparametric electrochemical analysis.

To enable a more quantitative assessment of FACILE 2.0's performance, four electroactive probes were analyzed $[Fe(CN)_6]^{3-/4-}$, $[Ru(NH_3)_6]^{2+/3+}$ (both reversible probes), AA and DA (non-reversible probes). The intentional selection of both reversible and irreversible redox systems validates the platform as a universal analytical instrument, independent of specific biosensing configurations. For a comprehensive comparison, identical experiments were conducted on commercial platforms (see Apparatus paragraph), providing a robust comparison across systems. The data summarized in Table 2 demonstrate satisfactory sensitivity and reproducibility for the Facile 2.0 platform, underscoring its reliability as a viable alternative to commercial systems. Notably, the repeatability, expressed as RSD% for $[Fe(CN)_6]^{3-/4-}$ was 8% for FACXILE 2.0, comparable with PalmSens 4.0 (10%), EmStat *Blue* (12%), and Autolab PGSTAT 12 (7%). Similarly, the limit of detection (LOD) for FACILE 2.0 was 0.7 μM, closely matching PalmSens 4.0 and EmStat *Blue* (0.6 μM) and slightly higher than Autolab PGSTAT 12 (0.5 μM). These results highlight the platform's excellent reliability across both reversible and irreversible systems.

3.3. Electrochemical performance of FACILE 2.0 in fluidic mode

Measurements were also conducted in fluidic mode by actuating the device's integrated peristaltic pump in a "start-stop" configuration. In this setup, the solvent flows from the sampling point to the electrode interface and then pauses briefly to allow for measurement.

This dynamic fluidic analysis ensures precise control over the timing of the solvent-electrode interaction, thereby enhancing sensitivity and accuracy in the electrochemical readouts. The electrochemical and operative results obtained by changing the flow rate or the electrochemical probe concentrations are reported in Fig. 5. A preliminary study was first conducted to identify the most suitable flow rate, balancing current intensity with signal reproducibility. This assessment involved testing various concentrations of the electroactive probe $[Fe(CN)_6]^{3-/4-}$ in combination with different flow rates. As shown in Fig. 5a, a flow rate of 1 mL/min was selected as the optimal condition. Building on this optimization, CA measurements were then performed-similarly to the static mode analysis, to evaluate the system's response to successive additions of the redox probe until electrode saturation was reached. This step aimed to assess the device's performance under demanding conditions, thus further validating the robustness and

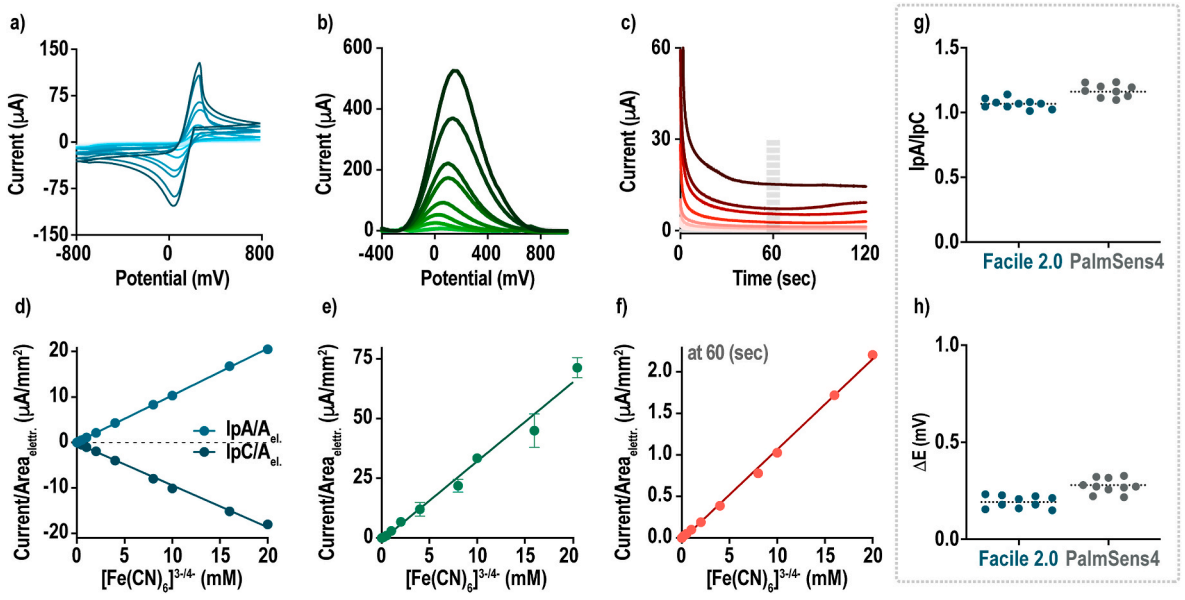

Fig. 3. Electrochemical performance of FACILE 2.0 under static conditions. (a-c) CV (scan rate of 50 mV/s, potential window from −800 to 800 mV), SWV (amplitude 0.2 V, frequency 30 Hz, potential window from −400 to 800 mV), and CA (260 mV, acquisition at 120 s) response for $[Fe(CN)_6]^{3-/4-}$ over 0 to 20 mM. (d-f) Corresponding calibration curves showing high linearity. (g,h) Comparison of Ip_A/Ip_C ratios and ΔE values from CV measurements between FACILE 2.0 and PalmSens 4.0, confirming comparable analytical performance. All measurements were performed in triplicate (n = 3).

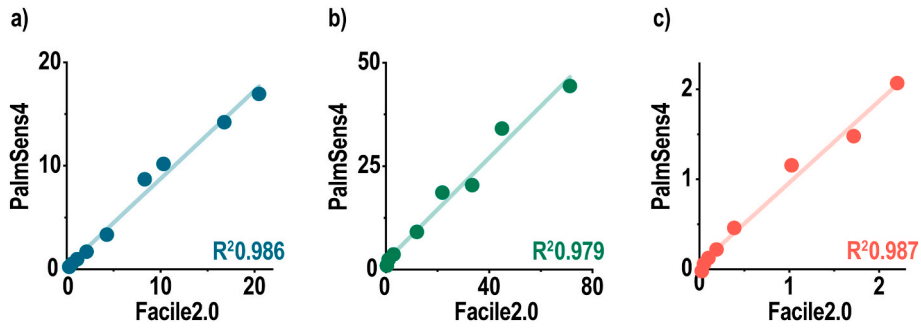

Fig. 4. Correlation analysis of electrochemical measurement between FACILE 2.0 and commercial instrument. (a) IpA from CV; (b) Peak current from SWV; (c) Current at 60 s from chronoamperometry. Strong linear correlation ($R^2 > 0.997$) confirms the reliability of FACILE 2.0 for reproducible electrochemical measurements.

Table 1
Electrochemical performance of FACILE 2.0

	CV_{anodic}	$CV_{cathodic}$	SWV	CA
Linear Function	y = 1.030x + 0.067	y = 0.921x – 0.209	y = 3.296x – 0.855	y = 0.109x – 0.023
Slope	1.030	−0.921	3.296	0.109
R^2	0.999	0.997	0.996	0.998

Table 2
Comparison of the static analytical performance of FACILE 2.0 with commercial potentiostats.

		PalmSens 4.0	Facile 2.0	Emstat	Autolab
$Fe^{2+/3+}$	LOD (μM)	0.6	0.7	0.6	0.5
	LOQ (μM)	1.8	2.2	1.8	1.6
	Sensitivity (mA/M cm^2)	8.7	10.1	8.7	7.5
	Reproducibility (RSD %)	10	8	12	7
$Hx^{2+/3+}$	LOD (μM)	2.3	3.6	2.7	1.6
	LOQ (μM)	6.8	10.9	7	5.1
	Sensitivity (mA/M cm^2)	5	5	5.8	4.2
	Reproducibility (RSD %)	8	8	10	7
AA	LOD (μM)	0.4	0.8	0.6	0.3
	LOQ (μM)	1.3	2.6	1.9	1.1
	Sensitivity (mA/M cm^2)	12.2	8.4	10.4	9.4
	Reproducibility (RSD %)	11	7	12	8
Dp	LOD (μM)	0.6	2.7	0.7	0.4
	LOQ (μM)	1.9	8.1	3.2	1.4
	Sensitivity (mA/M cm^2)	8.1	26.8	10.3	6.9
	Reproducibility (RSD %)	5	7	8	7

Note: $Fe^{2+/3+}$ and $Hx^{2+/3+}$ refer to $[Fe(CN)_6]^{3-/34-}$ and $[Ru(NH_3)_6]^{2+/3+}$, respectively.

reliability of the fluidic configuration. Fig. 5b–c depict the results obtained through these analyses.

3.4. Integration of the label-free electrochemical immunosensor for *P. aeruginosa* with the FACILE 2.0 potentiostat

As a proof-of-concept application in the biosensing field, a label-free electrochemical immunosensor for the detection of *Pseudomonas aeruginosa* was developed. For the initial analytical characterization, all experiments were performed under controlled conditions using 10 mM phosphate-buffered saline (PBS, pH 7.4) as the buffer. The immunosensor assembly, hence, the concentrations of the primary and secondary antibodies, as well as the conditions for immunocomplex formation, were systematically optimized and reported in SI (see Fig. S7). As illustrated in Fig. 6a, the immunocomplex forms upon exposure to serially diluted bacterial suspensions in the same buffer, promoting antigen–antibody interactions on the functionalized surface, and the interaction was carried out of 25 min at room temperature. Electrochemical sensing was performed using SWV in the presence of a 10 mM $[Fe(CN)_6]^{3-/4-}$ as redox probe. Increasing concentrations of the target bacterium led to a progressive decrease in the current signal, consistent with electrode surface blockage caused by immunocomplex formation. This response is governed by blocking access to the electrode (BAE) mechanism, a hallmark of label-free voltammetric immunosensors. Upon target recognition, the formation of the immunocomplex impedes the diffusion of the redox probe to the electrode surface, thereby attenuating electron transfer at the electrode–electrolyte interface [34]. The resulting calibration curve (Fig. 6b) displayed a typical sigmoidal trend as a function of the logarithm of bacterial concentration, in agreement with a molecular saturation model. The system exhibited good reproducibility, with an RSD% (n = 5) below 10% across independent replicates. The LOD was determined to be 170 CFU/mL, while the limit of quantification (LOQ) was found to be 200 CFU/mL. The working range extended from 220 to 8800 CFU/mL. Comparable results were obtained by using the PalmSens device for the sensing of the immunosensing platforms (data not reported). Subsequently, to further assess the robustness of the system under real-world conditions, the immunosensor was tested in tap water samples spiked with known concentrations of *P. aeruginosa*. The calibration curve obtained in this condition (Fig. 6c) confirmed the sensor's ability to selectively detect the pathogen even in the presence of a more complex matrix, with a LOD of 1000 CFU/mL and a linear response over the range of 1000 - 4300 CFU/mL. As observed previously in PBS, FACILE 2.0 delivered results that were in close agreement with those of the PalmSens 4.0 system, demonstrating comparable sensitivity and reproducibility. The analytical parameters remained within the relative standard deviation (RSD%, n = 5) range calculated across quintuplicate measurements, supporting the platform's consistency under real sample conditions. Finally, as shown in Fig. 6d, the specificity of the biosensor was evaluated in the presence of non-target microbial species. Three potential interferents were selected: *E. coli*, *S. aureus*, and *Hepatitis* A virus. The first two represent common bacterial species that may coexist with *P. aeruginosa* in clinical and environmental samples, while *Hepatitis A* virus, although virologically distinct, was included due to its frequent occurrence in water matrices. In all cases, the biosensor exhibited negligible cross-reactivity with all tested interferents, demonstrating strong target specificity and minimal signal interference. Indeed, no significant variations in the electrochemical signal were observed, confirming the high specificity of the system toward *P. aeruginosa*. These findings highlight the potential of using the FACILE 2.0 potentiostat with biofunctionalized

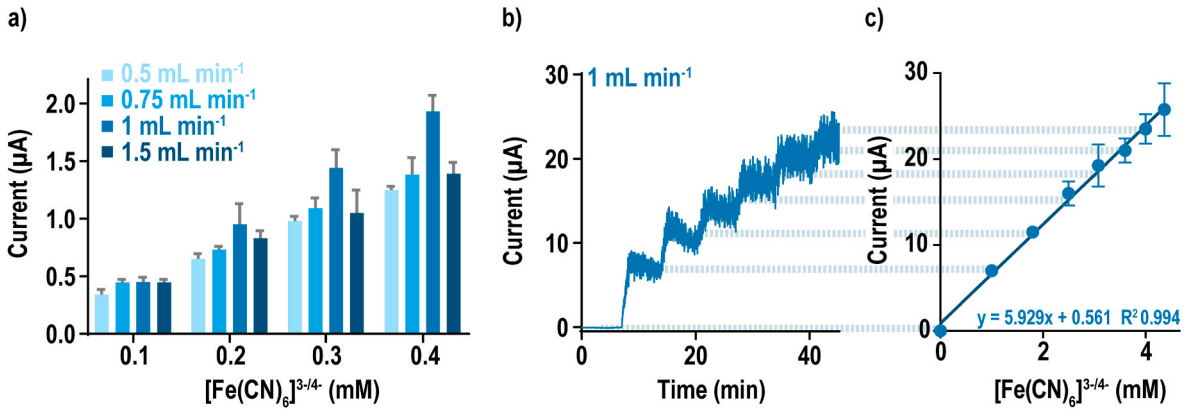

Fig. 5. Electrochemical performance of FACILE 2.0 in fluidic mode. (a) Optimization of flow rate (0.5, 0.75, 1, and 1.5 mL/min) and probe concentration using $[Fe(CN)_6]^{3-/4-}$ as a redox couple. (b) Chronoamperometric response at 1 mL/min with successive probe additions (from 0 to 4.4 mM). (c) Calibration curve under dynamic conditions, showing high signal linearity and reproducibility (RSD%<10).

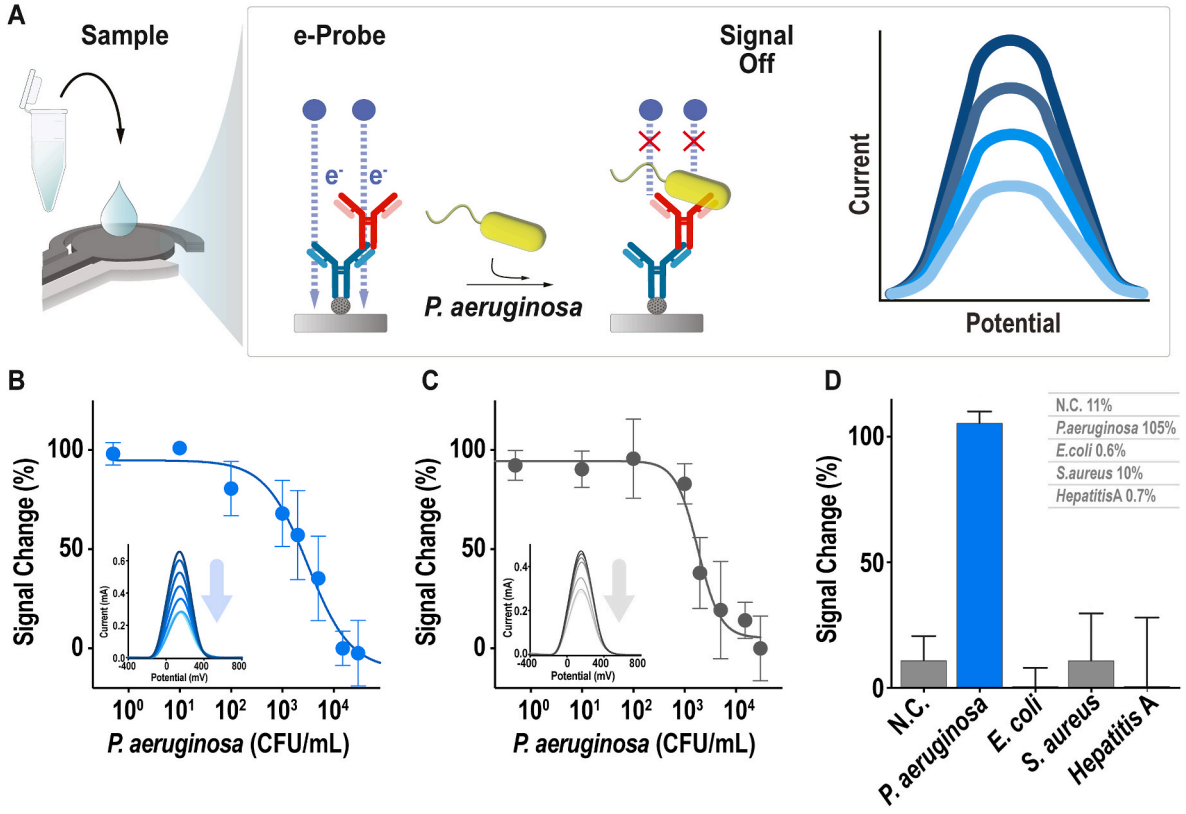

Fig. 6. Schematic description of label-free immunosensor for *P. aeruginosa*. (a) Schematic representation of the of label-free electrochemical immunosensor-based on Bio-SPEs for *P. aeruginosa* detection. Immunocomplex formation blocks redox probe access, suppressing the current signal. (b) Voltametric responses in 10 mM PBS buffer (pH 7.4) at increasing concentrations of *P. aeruginosa*, showing a sigmoidal calibration curve. (c) Calibration curve in untreated tap water spiked with known concentrations of *P. aeruginosa*, confirming system robustness. (d) Specificity assessment in the presence of non-target interfering species: the electrochemical signal remains unchanged, confirming the high selectivity of the system toward *P. aeruginosa*.

immunosensors as a rapid, sensitive, and reliable strategy for pathogen detection in complex environments. The use of nanostructured materials and targeted immobilization strategies proved essential for enhancing the overall performance of the sensor.

4. Conclusions and perspectives

This study presents FACILE 2.0, a next-generation portable potentiostat that bridges the gap between lab-grade analytical performance and field-ready electrochemical analysis. Its integration of dual-mode measurement capabilities (static and fluidic), embedded data processing, and programmable fluidic control represents a significant step toward compact and autonomous electroanalytical instrumentation.

The electrochemical validation demonstrated the reliability of the signal acquisition architecture across multiple techniques and operating conditions, confirming the platform's suitability for multiparametric measurements. The subsequent coupling with a biochar-based, label-free immunosensor for the detection of *Pseudomonas aeruginosa* further illustrated its applicability in complex real matrices, supporting its use in decentralized monitoring scenarios.

Beyond the specific biosensing application presented here, FACILE 2.0 constitutes a versatile electroanalytical workstation adaptable to a broad range of research, environmental, industrial, and educational contexts. Its modular architecture, integrated control interface, and compact design enable flexible implementation in both laboratory and field environments, providing a scalable foundation for future developments in portable electrochemical instrumentation.

Looking forward, FACILE 2.0 offers a flexible foundation for further enhancements, including multi-analyte detection, cloud-based data integration, and AI-assisted signal interpretation. Its open and modular design also supports adaptation to different targets and analytical needs, contributing to the development of portable electroanalytical systems for diverse scientific and industrial applications.

CRediT authorship contribution statement

Elisa Paialunga: Writing – review & editing, Writing – original draft, Validation, Supervision, Methodology, Investigation, Formal analysis, Data curation, Conceptualization. **Rocco Cancelliere:** Writing – review & editing, Writing – original draft, Visualization, Supervision, Methodology, Investigation, Formal analysis, Data curation, Conceptualization. **Antonio Licheri:** Methodology, Investigation, Formal analysis, Data curation. **Cosimo Micelli:** Software, Methodology, Investigation, Conceptualization. **Antonio Ceccarelli:** Resources. **Giulia Sarpi:** Investigation, Formal analysis. **David Albano:** Investigation, Formal analysis. **Benedetta Brugnoli:** Investigation. **Iolanda Francolini:** Writing – review & editing, Resources. **Laura Micheli:** Writing – review & editing, Supervision, Resources, Project administration, Methodology, Funding acquisition, Conceptualization. **Giuseppina Rea:** Writing – review & editing, Supervision, Resources, Project administration, Methodology, Funding acquisition, Conceptualization.

Funding sources

This work was supported by the Regione Lazio funded project FACILE. “Development of a sensitive and versatile electrochemical platform for advanced biosensor applications in the environmental and agribusiness sectors”, grant n. 85-2017-15256; MUR-PRIN 2022 PNRR Decreto Direttoriale n. 1409 del 14-9-2022, project “Dress the future: novel combined wearable integrated system (Stargate)” project n° P2022CZA3P; Lazio Innova “Intervento per il rafforzamento della ricerca e innovazione nel Lazio” PhD Program XXVII Cycle (L.R. 13/2008); MUR Dipartimento di Eccellenza 2023-27 project X-CHEM “eXpanding CHEMistry: implementing excellence in research and teaching”.

Declaration of competing interest

The authors declare that they have no known competing financial interests or personal relationships that could have appeared to influence the work reported in this paper.

Acknowledgements

The authors gratefully acknowledge Massimiliano Catricalà and Antonello Ranieri (Institute of Crystallography, CNR) for their valuable technical support in testing and maintenance of the electronic systems; SANA srl (Frosinone, IT) for the supply of the pathogens, for the control analysis of the title of their suspensions (see Materials and Methods) and for allowing the authors to carry out the measurements in controlled and healthy conditions.

Appendix A. Supplementary data

Supplementary data to this article can be found online at https://doi.org/10.1016/j.talanta.2026.129761.

Data availability

No data was used for the research described in the article.

References

[1] M.M. Shanbhag, G. Manasa, R.J. Mascarenhas, K. Mondal, N.P. Shetti, Fundamentals of bio-electrochemical sensing, Chem. Eng. J. Adv. 16 (2023) 100516, https://doi.org/10.1016/j.ceja.2023.100516.
[2] R. Cancelliere, E. Paialunga, A. Grattagliano, L. Micheli, Label-free electrochemical immunosensors: a practical guide, TrAC, Trends Anal. Chem. 180 (2024) 117949, https://doi.org/10.1016/j.trac.2024.117949.
[3] A. Ainla, M.P.S. Mousavi, M.-N. Tsaloglou, J. Redston, J.G. Bell, M.T. Fernández-Abedul, G.M. Whitesides, Open-source potentiostat for wireless electrochemical detection with smartphones, Anal. Chem. 90 (2018) 6240–6246, https://doi.org/10.1021/acs.analchem.8b00850.
[4] V. Bianchi, A. Boni, S. Fortunati, M. Giannetto, M. Careri, I. De Munari, A Wi-Fi cloud-based portable potentiostat for electrochemical biosensors, IEEE Trans. Instrum. Meas. 69 (2020) 3232–3240, https://doi.org/10.1109/TIM.2019.2928533.
[5] S.C.-H. Lee, P.J. Burke, NanoStat: an open source, fully wireless potentiostat, Electrochim. Acta 422 (2022) 140481, https://doi.org/10.1016/j.electacta.2022.140481.
[6] F.A. Assaig, T.S. Gunawan, A.N. Nordin, R. Ab Rahim, Z. Mohd Zain, R. Mohd Zain, F. Arifin, Development and evaluation of a high-performance electrochemical potentiostat-based desktop application for rapid SARS-CoV-2 testing, Int. J. E Enterpren. Innovat. 11 (2023) 349–365, https://doi.org/10.52549/ijeei.v11i2.4645.
[7] S. Abdullah, S. Tonello, M. Borghetti, E. Sardini, M. Serpelloni, Potentiostats for protein biosensing: design considerations and analysis on measurement characteristics, J. Sens. 2019 (2019) 1–20, https://doi.org/10.1155/2019/6729329.
[8] P. Aryal, C. Hefner, B. Martinez, C.S. Henry, Microfluidics in environmental analysis: advancements, challenges, and future prospects for rapid and efficient monitoring, Lab Chip 24 (2024) 1175–1206, https://doi.org/10.1039/D3LC00871A.
[9] N. Kalita, S. Gogoi, S.D. Minteer, P. Goswami, Advances in bioelectrode design for developing electrochemical biosensors, ACS Meas. Sci. Au 3 (2023) 404–433, https://doi.org/10.1021/acsmeasuresciau.3c00034.
[10] A.F.D. Cruz, N. Norena, A. Kaushik, S. Bhansali, Biosens. Bioelectron. 62 (2014) 249.
[11] J.T.C. Barragan, L.T. Kubota, Minipotentiostat controlled by smartphone on a micropipette: a versatile, portable, agile and accurate tool for electroanalysis, Electrochim. Acta 341 (2020) 136048, https://doi.org/10.1016/j.electacta.2020.136048.
[12] H. Duan, S. Peng, S. He, S. Tang, K. Goda, C.H. Wang, M. Li, Wearable electrochemical biosensors for advanced healthcare monitoring, Adv. Sci. 12 (2025) 2411433, https://doi.org/10.1002/advs.202411433.
[13] Z. Zhang, H. Karimi-Maleh, In situ synthesis of label-free electrochemical aptasensor-based sandwich-like AuNPs/PPy/Ti3C2Tx for ultrasensitive detection of lead ions as hazardous pollutants in environmental fluids, Chemosphere 324 (2023) 138302, https://doi.org/10.1016/j.chemosphere.2023.138302.
[14] X. Xu, X. Li, J. Miao, L. Liu, X. Huang, Q. Wei, W. Cao, A dual-mode label-free electrochemical immunosensor for ultrasensitive detection of procalcitonin based on g-C_3N_4-$NiCo_2S_4$-CNTs-Ag NPs, Analyst 146 (2021) 3169–3176, https://doi.org/10.1039/D1AN00372K.
[15] S. Akbari Nakhjavani, H. Mirzajani, S. Carrara, M.C. Onbaşlı, Advances in biosensor technologies for infectious diseases detection, TrAC, Trends Anal. Chem. 180 (2024) 117979, https://doi.org/10.1016/j.trac.2024.117979.
[16] P. Cao, D. Fleming, D.A. Moustafa, S.K. Dolan, K.H. Szymanik, W.K. Redman, A. Ramos, F.L. Diggle, C.S. Sullivan, J.B. Goldberg, K.P. Rumbaugh, M. Whiteley, A Pseudomonas aeruginosa small RNA regulates chronic and acute infection, Nature 618 (2023) 358–364, https://doi.org/10.1038/s41586-023-06111-7.
[17] L.A. Meirelles, E. Vayena, A. Debache, E. Schmidt, T. Rossy, T. Distler, V. Hatzimanikatis, A. Persat, Pseudomonas aeruginosa faces a fitness trade-off between mucosal colonization and antibiotic tolerance during airway infection, Nat. Microbiol. (2024), https://doi.org/10.1038/s41564-024-01842-3.
[18] S. Qin, W. Xiao, C. Zhou, Q. Pu, X. Deng, L. Lan, H. Liang, X. Song, M. Wu, Pseudomonas aeruginosa: pathogenesis, virulence factors, antibiotic resistance, interaction with host, technology advances and emerging therapeutics, Signal Transduct. Targeted Ther. 7 (2022) 199, https://doi.org/10.1038/s41392-022-01056-1.
[19] A.L. Swart, B.-J. Laventie, R. Sütterlin, T. Junne, L. Lauer, P. Manfredi, S. Jakonia, X. Yu, E. Karagkiozi, R. Okujava, U. Jenal, Pseudomonas aeruginosa breaches respiratory epithelia through goblet cell invasion in a microtissue model, Nat. Microbiol. 9 (2024) 1725–1737, https://doi.org/10.1038/s41564-024-01718-6.
[20] F. Kunisch, C. Campobasso, J. Wagemans, S. Yildirim, B.K. Chan, C. Schaudinn, R. Lavigne, P.E. Turner, M.J. Raschke, A. Trampuz, M. Gonzalez Moreno, Targeting Pseudomonas aeruginosa biofilm with an evolutionary trained bacteriophage cocktail exploiting phage resistance trade-offs, Nat. Commun. 15 (2024) 8572, https://doi.org/10.1038/s41467-024-52595-w.
[21] E. Rossi, R. La Rosa, J.A. Bartell, R.L. Marvig, J.A.J. Haagensen, L.M. Sommer, S. Molin, H.K. Johansen, Pseudomonas aeruginosa adaptation and evolution in

patients with cystic fibrosis, Nat. Rev. Microbiol. 19 (2021) 331–342, https://doi.org/10.1038/s41579-020-00477-5.
[22] WHO Bacterial Priority Pathogens List 2024: Bacterial Pathogens of Public Health Importance, to Guide Research, Development, and Strategies to Prevent and Control Antimicrobial Resistance, first ed., World Health Organization, Geneva, 2024.
[23] S. Baidya, S. Sharma, S.K. Mishra, H.P. Kattel, K. Parajuli, J.B. Sherchand, Biofilm formation by pathogens causing ventilator-associated pneumonia at intensive care units in a tertiary care hospital: an armor for refuge, BioMed Res. Int. 2021 (2021) 1–10, https://doi.org/10.1155/2021/8817700.
[24] M.F. Moradali, S. Ghods, B.H.A. Rehm, Pseudomonas aeruginosa lifestyle: a paradigm for adaptation, survival, and persistence, Front. Cell. Infect. Microbiol. 7 (2017), https://doi.org/10.3389/fcimb.2017.00039.
[25] M.J. Figueras, J.J. Borrego, New perspectives in monitoring drinking water microbial quality, IJERPH 7 (2010) 4179–4202, https://doi.org/10.3390/ijerph7124179.
[26] A.M. Algammal, M. Mabrok, E. Sivaramasamy, F.M. Youssef, M.H. Atwa, A.W. El-kholy, H.F. Hetta, W.N. Hozzein, Emerging MDR-Pseudomonas aeruginosa in fish commonly harbor oprL and toxA virulence genes and blaTEM, blaCTX-M, and tetA antibiotic-resistance genes, Sci. Rep. 10 (2020) 15961, https://doi.org/10.1038/s41598-020-72264-4.
[27] K.D. Mena, C.P. Gerba, Risk assessment of Pseudomonas aeruginosa in water, in: D. M. Whitacre (Ed.), Reviews of Environmental Contamination and Toxicology, vol 201, Springer US, Boston, MA, 2009, pp. 71–115, https://doi.org/10.1007/978-1-4419-0032-6_3.
[28] M. Khodaparast, D. Sharley, S. Marshall, T. Beddoe, Advances in point-of-care and molecular techniques to detect waterborne pathogens, npj Clean Water 7 (2024) 74, https://doi.org/10.1038/s41545-024-00368-9.
[29] J.M. Janda, S.L. Abbott, 16S rRNA gene sequencing for bacterial identification in the diagnostic laboratory: pluses, perils, and pitfalls, J. Clin. Microbiol. 45 (2007) 2761–2764, https://doi.org/10.1128/JCM.01228-07.
[30] Y.-L. Oon, Y.-S. Oon, M. Ayaz, M. Deng, L. Li, K. Song, Waterborne pathogens detection technologies: advances, challenges, and future perspectives, Front. Microbiol. 14 (2023) 1286923, https://doi.org/10.3389/fmicb.2023.1286923.
[31] S. Anuj, D.M. Whiley, Pseudomonas aeruginosa, in: M. Schuller, T.P. Sloots, G. S. James, C.L. Halliday, I.W.J. Carter (Eds.), PCR for Clinical Microbiology, Springer Netherlands, Dordrecht, 2010, pp. 191–195, https://doi.org/10.1007/978-90-481-9039-3_24.
[32] H. Maeda, C. Fujimoto, Y. Haruki, T. Maeda, S. Kokeguchi, M. Petelin, H. Arai, I. Tanimoto, F. Nishimura, S. Takashiba, Quantitative real-time PCR using TaqMan and SYBR green for *Actinobacillus actinomycetemcomitans* , *Porphyromonas gingivalis* , *Prevotella intermedia* , *tetQ* gene and total bacteria, FEMS Immunol. Med. Microbiol. 39 (2003) 81–86, https://doi.org/10.1016/S0928-8244(03)00224-4.
[33] A. Chamorro-Garcia, A. Merkoçi, Nanobiosensors in diagnostics, Nanobiomedicine (Rij.) 3 (2016) 1849543516663574, https://doi.org/10.1177/1849543516663574.
[34] R. Cancelliere, P. Mele, L. Bartolucci, S. Cordiner, W. Da Silva Freitas, C. Mazzuca, B. Mecheri, L. Micheli, V. Mulone, E. Paialunga, L. Severini, Mutual interaction of pyrolysis operating conditions and surface morphology for the electrochemical performance of biochar-modified screen-printed electrodes, J. Environ. Chem. Eng. (2025) 115477, https://doi.org/10.1016/j.jece.2025.115477.
[35] L. Micheli, A. Fasoli, A. Attar, D.T. Donia, M. Divizia, A. Amine, G. Palleschi, P. A. Salazar Carballo, D. Moscone, An ELIME assay for hepatitis A virus detection, Talanta 234 (2021) 122672, https://doi.org/10.1016/j.talanta.2021.122672.
[36] C. D'Agostino, R. Cancelliere, A. Ceccarelli, D. Moscone, L. Cozzi, G. La Rosa, E. Suffredini, L. Micheli, Evaluation of an enzyme-linked magnetic electrochemical assay for Hepatitis a virus detection in drinking and vegetable processing water, Chemosensors 12 (2024) 188, https://doi.org/10.3390/chemosensors12090188.
[37] R. Cancelliere, A. Di Tinno, A. Cataldo, S. Bellucci, S. Kumbhat, L. Micheli, Nafion-based Label-free immunosensor as a reliable warning system: the case of AFB1 detection in cattle feed, Microchem. J. (2023) 108868, https://doi.org/10.1016/j.microc.2023.108868.